

Supporting Information

Lanthanide MOFs for Inducing Molecular Chirality of Achiral Stilbazolium with Strong Circularly Polarized Luminescence and Efficient Energy Transfer for Color Tuning

Min Zeng,^{a,c†} Ang Ren,^{a,c†} Wubin Wu,^{a,c} Yongsheng Zhao,^{a,c*} Chuanlang Zhan^{a,b,c*} and Jiannian Yao^{a,c*}

^a Beijing National Laboratory for Molecular Sciences, CAS Key Laboratory of Photochemistry, Institute of Chemistry, Chinese Academy of Sciences, Beijing, 100190, P.R. China.

^b Key Laboratory of Excitonic Materials Chemistry and Devices (EMC&D), College of Chemistry and Environmental Science, Inner Mongolia Normal University, Huhhot 010022, China.

^c University of Chinese Academy of Sciences, Beijing, 100049, P. R. China.

Corresponding Authors: clzhan@iccas.ac.cn (C.Z.), yszhao@iccas.ac.cn, jnyao@iccas.ac.cn (J.Y.).

Contents

1. EXPERIMENTAL SECTION	5
1.1 Materials and Reagents	5
1.2 Synthesis of TbBTC	5
1.3 Synthesis of DSM@TbBTC	5
1.4 TbBTC chiral separation into P- and M-TbBTC.....	5
1.5 Synthesis of MOF-5	5
1.6 Synthesis of DSM@MOF-5	6
1.7 Synthesis of DSM@TbBTC-X	6
1.8 Structural Characterization.....	6
1.9 Spectroscopic measurements	6
1.10 Density Functional Theory (DFT) calculations.....	7
1.11 Calculations of DSM content in DSM@TbBTC.....	7
2. SUPPORTING FIGURES	8
Fig. S1. Chiral separation of TbBTC. Schematic diagram of chiral separation of racemic mixture of TbBTC into right-hand P-(+)-TbBTC-a and -b and left-hand M(-)-TbBT-c and -d, respectively.	8
Fig. S2. 3D structure of (a) TbBTC-a, (b) TbBTC-b, (c) TbBTC-c and (d) TbBTC-d viewing along the c-axis.....	8
Fig. S3. Simulated and experimental PXRD patterns of four types of TbBTC: -a, -b, -c and -d, respectively.	9
Fig. S4. Schematic view of the helical alignment of Tb ³⁺ ion along the crystallographic axis for four types of TbBTC: -a (a), -b (b), -c (c) and -d (d), respectively.	9
Fig. S5. PXRD patterns and photoluminescence images of TbBTC and DSM@TbBTC: Photoluminescence images (inserts) show that upon 355 nm excitation, TbBTC and DSM@TbBTC emit green and orange-red light, respectively. The orange-red emission is	

homogenously distributed throughout whole the microrod, suggesting successful loading of DSM into the cavities of TbBTC.....	10
Fig. S6 (a) PXRD patterns of simulated MOF-5 and experimental MOF-5, (b) Solid-state CPL spectrum of DSM@MOF-5 under 514 nm excitation. Insert: 3D pore structure of MOF-5.....	10
Fig. S7. Photoluminescence image of DSM@P-(+)-TbBTC under 514 nm continuous wave laser excitation.....	11
Fig. S8. Solid and solution in CD ₂ Cl ₂ Raman spectra of DSM and the Deuterated dichloromethane.	11
Fig. S9. Absorption (Abs) and emission (EM) spectra of Tb ³⁺ and DSM, showing well overlap of the fluorescence spectrum of Tb ³⁺ and absorption spectrum of DSM, featuring energy transfer from Tb ³⁺ to DSM. TbBTC exhibits four Tb ³⁺ characteristic peaks at 487, 544, 583 and 622 nm, which are attributed to ⁵ D ₄ → ⁷ F ₆ , ⁵ D ₄ → ⁷ F ₅ , ⁵ D ₄ → ⁷ F ₄ and ⁵ D ₄ → ⁷ F ₃ , respectively. Fluorescence of DSM in DSM@TbBTC appears around 615 nm.....	12
Fig. S10. Solid-state emission spectra of DSM, TbBTC, DSM-TbBTC (a thoroughly grinded mixture of DSM and TbBTC), and DSM@TbBTC under 355 nm excitation at room temperature.	12
3. SUPPORTING TABLES.....	13
Table S1. Crystal data and structure refinement for TbBTC-a.	13
Table S2. Bond Lengths for TbBTC-a.....	13
Table S3. Crystal data and structure refinement for TbBTC-b.....	14
Table S4. Bond Lengths for TbBTC-b.	15
Table S5. Crystal data and structure refinement for TbBTC-c.	15
Table S6. Bond Lengths for TbBTC-c.....	16
Table S7. Crystal data and structure refinement for TbBTC-d.....	17
Table S8. Bond Lengths for TbBTC-d.	17
Table S9. Crystal data and structure refinement for DSM@P-(+)-TbBTC after removing the DSM molecule.....	18

Table S10. Bond Lengths for DSM@P-(+)-TbBTC after removing the DSM molecule.	19
Table S11. Crystal data and structure refinement for DSM.	19
Table S12. Bond Lengths for DSM.	20
Table. S13 The C and N contents in DSM@TbBTC-X determined by Element Analysis.	20
Table. S14 Fluorescent lifetimes, energy transfer efficiency, quantum yield and CIE coordinates of TbBTC and DSM@TbBTC-X	21

1. EXPERIMENTAL SECTION

1.1 Materials and Reagents

Analytically pure $\text{Tb}(\text{NO}_3)_3 \cdot 6\text{H}_2\text{O}$, $\text{Zn}(\text{NO}_3)_2 \cdot 6\text{H}_2\text{O}$, 1,3,5-benzenetricarboxylic acid (H_3BTC), terephthalic acid (H_2BDC), (4-p-(dimethylamino)styryl)-1-methylpyridinium iodide (DSM), (S)-(+)-2-amino-1-butanol, (R)-(-)-2-amino-1-butanol, HNO_3 , CH_2Cl_2 , ethanol (EtOH) and N, N-dimethylformamide (DMF) were obtained from commercial sources and used directly without further purification.

1.2 Synthesis of TbBTC

A mixture of $\text{Tb}(\text{NO}_3)_3 \cdot 6\text{H}_2\text{O}$ (0.15 mmol), 1,3,5-benzenetricarboxylic acid (H_3BTC , 0.5 mmol), DMF (6 mL) and H_2O (4 mL) were sealed in a 20 mL of vial and then ultrasonic treated for 10 min at room temperature. The resulting solution was heated at 70°C for 4 hours. After cooling to room temperature, the obtained white-transparent crystals were washed two times with EtOH and two times with CH_2Cl_2 . Then, the crystals were dried at 60°C for 4 hours for the further encapsulation process.

1.3 Synthesis of DSM@TbBTC

As-synthesized crystalline TbBTC was soaked in 10 mL CH_2Cl_2 solution of DSM (0.1 mM) at room temperature and absorption equilibrium achieved after 5 days. The obtained red crystals were washed several times with EtOH until no DSM was detected in the filtrate.

1.4 TbBTC chiral separation into P- and M-TbBTC

P-(+)- and M-(-)-TbBTC were prepared according to a previously report. Briefly, 0.15mmol $\text{Tb}(\text{NO}_3)_3 \cdot 6\text{H}_2\text{O}$, 0.5 mmol 1,3,5-benzenetricarboxylic acid (H_3BTC), 9 mL DMF and 6 mL H_2O were mixed and ultrasonic treated until completely dissolved. Then, 1 mL (S)-(+)-2-amino-1-butanol [or (R)-(-)-2-amino-1-butanol] was introduced into above solution. After 10 minutes stirring, a small amount of HNO_3 was added until it becomes transparent. Subsequently, the resulted solution was heated 8 h under 100°C .

1.5 Synthesis of MOF-5

A mixture of $\text{Zn}(\text{NO}_3)_2 \cdot 6\text{H}_2\text{O}$ (1 mmol), terephthalic acid (H_2BDC , 0.5 mmol), DMF

(20 mL) and H₂O (0.5 mL) were sealed in a 25 mL of vial and then ultrasonic treated until completely dissolved. The resulting solution was heated at 120°C for 8 hours. The obtained white crystals were washed three times with EtOH and dried at 60 °C for 4 hours for the further encapsulation process.

1.6 Synthesis of DSM@MOF-5

MOF-5 was soaked in 10 mL CH₂Cl₂ solution of DSM (0.1 mM) for 5 days. The obtained red crystals were washed three times with EtOH.

1.7 Synthesis of DSM@TbBTC-X

As-prepared TbBTC was soaked in 10 mL CH₂Cl₂ solution of DSM with different concentrations (0.0025, 0.005, 0.01, 0.05 and 0.1 mM) at room temperature for 2 days. The different red crystals (named as DSM@TbBTC-X, X= 1, 2, 3, 4 and 5) were obtained and washed several times with EtOH to remove the DSM on the surface.

1.8 Structural Characterization

The single-crystal X-ray diffraction measurements of TbBTC were tested on a Rigaku MM007HF Saturn724+ diffractometer by using Mo K α radiation ($\lambda = 0.71073 \text{ \AA}$) in a ω -scan fashion at 173.15 K. For a total of ten trials, four types of crystal structures (TbBTC-a, TbBTC-b, TbBTC-c and TbBTC-d) were obtained. Powder X-ray diffraction (PXRD) data of the samples were recorded from a Rigaku D/max 2500 diffractometer with Cu K α radiation ($\lambda = 1.5418 \text{ \AA}$). Simulated PXRD of TbBTC-a, TbBTC-b, TbBTC-c and TbBTC-d were calculated by *Mercury* software using the crystallographic data (CIF). The C, H and N microanalyses were carried on a thermal Flash EA 1112 elemental analyzer. The fluorescence microscope images were obtained on an Olympus IX83 fluorescence microscope using a xenon lamp (325-375 nm) as excitation source. Raman spectrum were recorded using a HORIBA LabRAM HR Evolution laser microscopic confocal Raman spectrometer equipped with a 50 \times objective and a 785 nm laser (power= 10 mW) and Thermo Fisher DXRxi Micro Raman imaging spectrometer with a 10 \times objective and a 780 nm laser (power= 6.0 mW).

1.9 Spectroscopic measurements

Ultraviolet-visible (UV-vis) spectra were performed on a Hitachi U-3010 ultraviolet

spectrophotometer in the range of 300-800 nm. Photoluminescence spectroscopy (PL) were tested on a Hitachi F-7000 fluorescence spectrometer. PL lifetimes (τ) of measured on a HORIBA Delta Flex fluorescent lifetime analyzer. The fluorescence quantum efficiency (PLQY) values at room temperature were estimated using integrating sphere (F-3018, Edinburgh) accessory in a Nanolog FL3-2iHR fluorescence spectrometer. The CD spectra were measured on JASCO J-1500 with the refractive mode using the powder CD unit and FDCD detector. The circularly polarized luminescence (CPL) spectrum was measured on a JASCO CPL-300 spectrometer with the powder samples. Before UV-vis, PL, PLQY, PL lifetimes or PLQY testing, solid-state powder samples were sandwiched between two quartz plates. For micro-area CPL measurement, DSM@P-(+)-TbBTC single-crystal microrod was selected as the example. After being filtered by a band-pass filter (514 ± 12.5 nm), a continuous laser at 514 nm excited the single crystal microrod and emitted CPL at the tip. The CPL passed through 550 nm long-pass filter, changed into linear polarized light at $\pm 45^\circ$ by using $\lambda/4$ waveplate. Subsequently, by rotating the linear polarizer to different angle θ ($0-360^\circ$), the PL intensities of the $+45^\circ$ and -45° linear polarized light can be recorded per 30° .

1.10 Density Functional Theory (DFT) calculations

Potential energy surface calculation: utilizing B3lyp method at the level of 6-31G(d,p), the molecular geometry of DSM was optimized. Based on the optimized geometry, the potential energy surface rigid scans have been calculated with the B3lyp method at the level of 6-31G(d,p).

HOMO-LUMO gap calculation: based on the geometry of 10° twisted DSM, the frontier molecular orbitals were obtained on the basic set of B3lyp/6-31G. All the Quantum chemical calculations were completed in Gaussian 09 program package.

1.11 Calculations of DSM content in DSM@TbBTC

Chemical formula for DSM and TbBTC is $C_{16}H_{19}N_2I$ and $C_9H_5O_7Tb$, respectively. Assuming the molar number of C and N is x and y, which can be determined by C, H, N Element Analysis. Thus, the molar number of DSM is $y/2$, the molar number of TbBTC is $(x-8y)/9$. The molar ratio of TbBTC to DSM can be calculated from the formula

$(x-8y)/4.5y$. The concentration of DSM in TbBTC can be calculated from the formula

$$C = \frac{\frac{y}{2} \times M_1}{\frac{y}{2} \times M_1 + (x-8y)M_2/9},$$

where M_1 and M_2 represent the relative molar mass of DSM and TbBTC, respectively.

2. SUPPORTING FIGURES

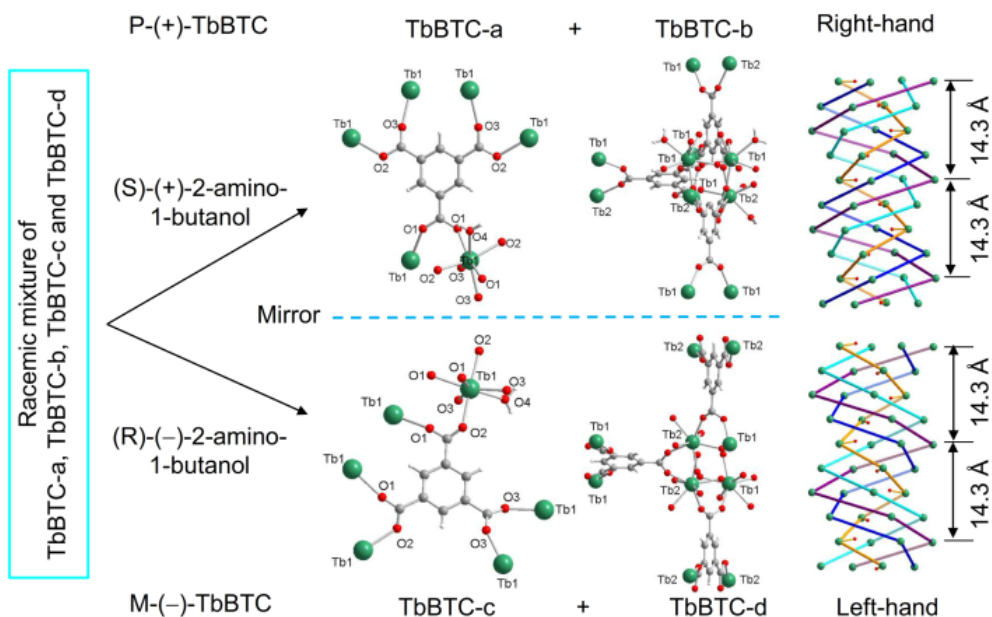


Fig. S1. Chiral separation of TbBTC. Schematic diagram of chiral separation of racemic mixture of TbBTC into right-hand P-(+)-TbBTC-a and -b and left-hand M-(-)-TbBTC-c and -d, respectively.

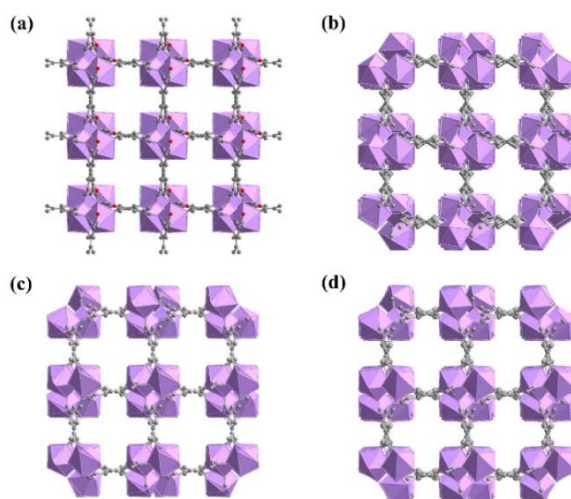


Fig. S2. 3D structure of (a) TbBTC-a, (b) TbBTC-b, (c) TbBTC-c and (d) TbBTC-d viewing along the c-axis.

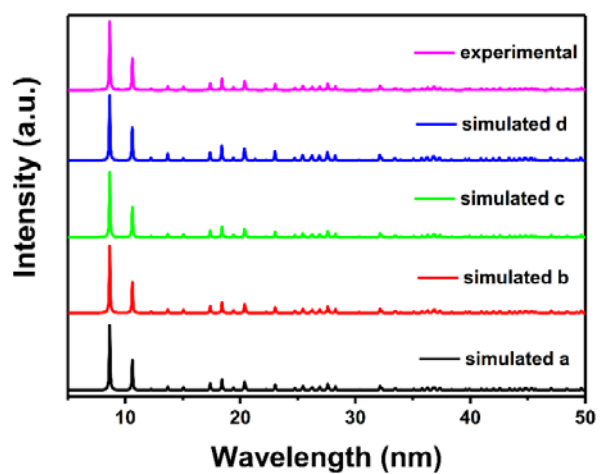


Fig. S3. Simulated and experimental PXRD patterns of four types of TbBTC: -a, -b, -c and -d, respectively.

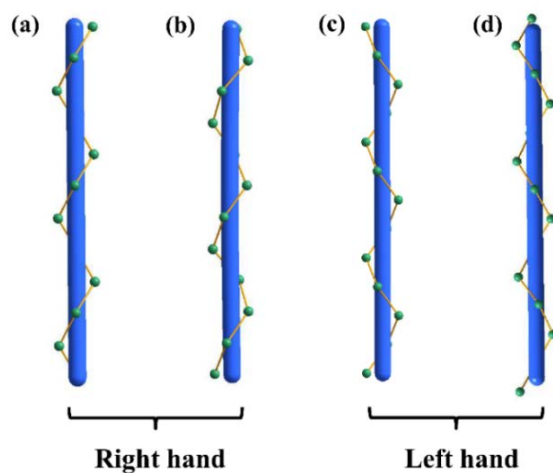


Fig. S4. Schematic view of the helical alignment of Tb^{3+} ion along the crystallographic axis for four types of TbBTC: -a (a), -b (b), -c (c) and -d (d), respectively.

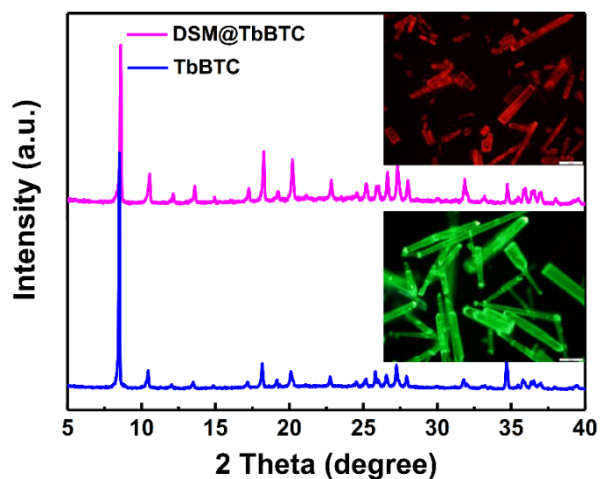


Fig. S5. PXRD patterns and photoluminescence images of TbBTC and DSM@TbBTC: Photoluminescence images (inserts) show that upon 355 nm excitation, TbBTC and DSM@TbBTC emit green and orange-red light, respectively. The orange-red emission is homogeneously distributed throughout whole the microrod, suggesting successful loading of DSM into the cavities of TbBTC.

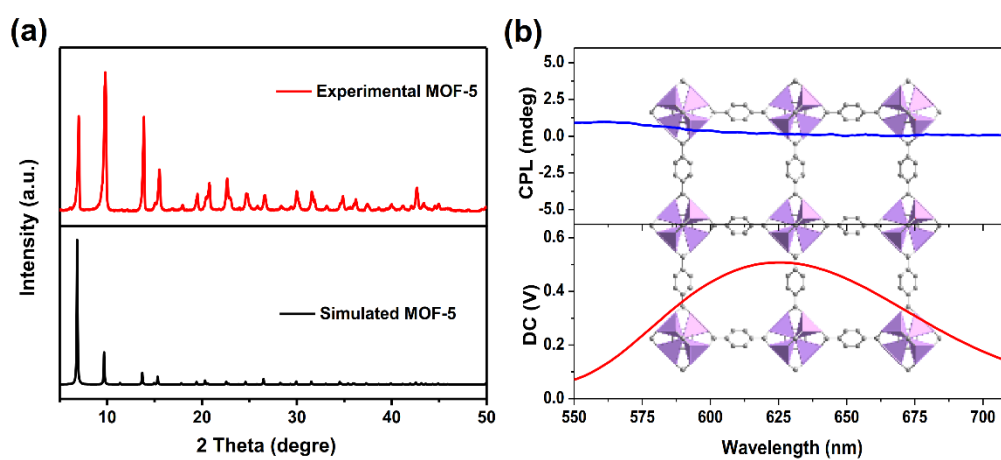


Fig. S6 (a) PXRD patterns of simulated MOF-5 and experimental MOF-5, (b) Solid-state CPL spectrum of DSM@MOF-5 under 514 nm excitation. Insert: 3D pore structure of MOF-5.



Fig. S7. Photoluminescence image of DSM@P-(+)-TbBTC under 514 nm continuous wave laser excitation.

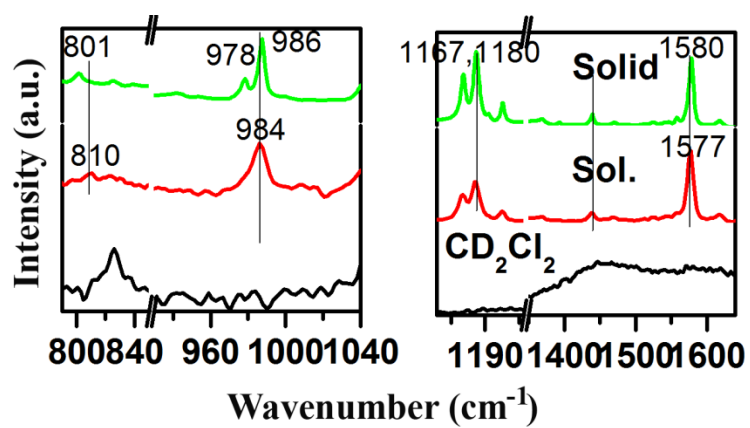


Fig. S8. Solid and solution in CD₂Cl₂ Raman spectra of DSM and the Deuterated dichloromethane.

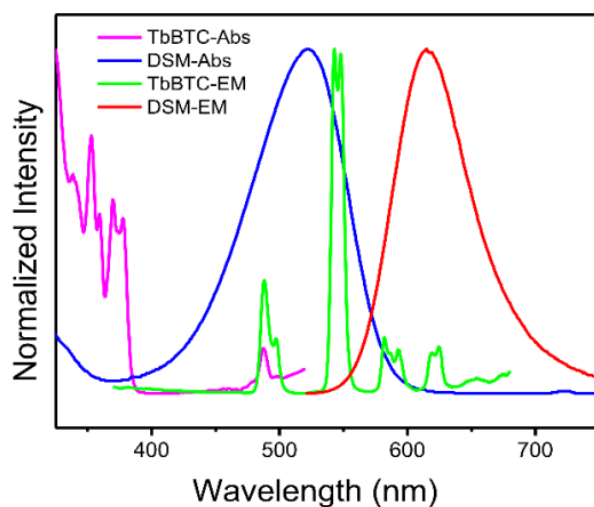


Fig. S9. Absorption (Abs) and emission (EM) spectra of Tb^{3+} and DSM, showing well overlap of the fluorescence spectrum of Tb^{3+} and absorption spectrum of DSM, featuring energy transfer from Tb^{3+} to DSM. TbBTC exhibits four Tb^{3+} characteristic peaks at 487, 544, 583 and 622 nm, which are attributed to $^5\text{D}_4 \rightarrow ^7\text{F}_6$, $^5\text{D}_4 \rightarrow ^7\text{F}_5$, $^5\text{D}_4 \rightarrow ^7\text{F}_4$ and $^5\text{D}_4 \rightarrow ^7\text{F}_3$, respectively. Fluorescence of DSM in DSM@TbBTC appears around 615 nm.

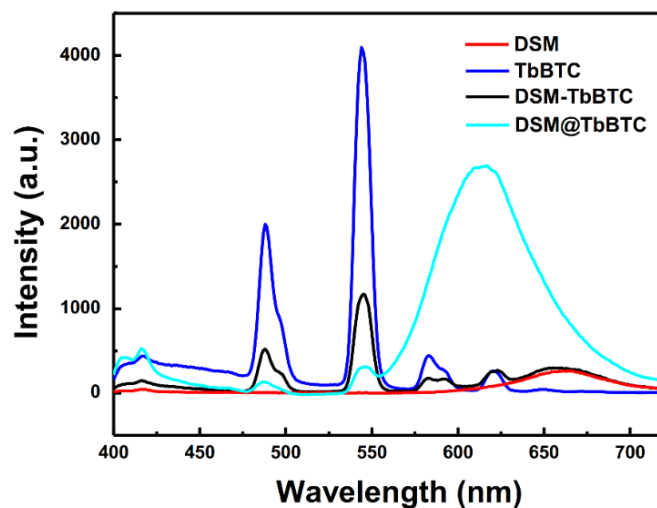


Fig. S10. Solid-state emission spectra of DSM, TbBTC, DSM-TbBTC (a thoroughly grinded mixture of DSM and TbBTC), and DSM@TbBTC under 355 nm excitation at room temperature.

3. SUPPORTING TABLES

Table S1. Crystal data and structure refinement for TbBTC-a.

Empirical formula	C ₉ H ₅ O ₇ Tb
Formula weight	384.05
Temperature/K	170.00(10)
Crystal system	tetragonal
Space group	P4 ₁ 22
a/Å	10.27740(10)
b/Å	10.27740(10)
c/Å	14.32360(10)
α/°	90
β/°	90
γ/°	90
Volume/Å ³	1512.93(3)
Z	4
ρ _{calc} /cm ³	1.686
μ/mm ⁻¹	23.171
F(000)	720.0
Crystal size/mm ³	0.2 × 0.053 × 0.05
Radiation	CuKα (λ = 1.54184)
2θ range for data collection/°	8.604 to 150.934
Index ranges	-12 ≤ h ≤ 12, -11 ≤ k ≤ 11, -17 ≤ l ≤ 17
Reflections collected	14174
Independent reflections	1537 [R _{int} = 0.0485, R _{sigma} = 0.0182]
Data/restraints/parameters	1537/117/119
Goodness-of-fit on F ²	1.106
Final R indexes [I ≥ 2σ (I)]	R ₁ = 0.0308, wR ₂ = 0.0766
Final R indexes [all data]	R ₁ = 0.0311, wR ₂ = 0.0769
Largest diff. peak/hole / e Å ⁻³	0.72/-1.26
Flack parameter	0.027(17)

Table S2. Bond Lengths for TbBTC-a.

Atom	Atom	Length/Å	Atom	Atom	Length/Å
Tb1	O1 ¹	2.330(17)	C2	C3 ⁶	1.41(3)
Tb1	O1	2.330(17)	C2	C3	1.41(3)
Tb1	O2 ²	2.310(7)	C3	C4	1.393(10)
Tb1	O2 ³	2.310(7)	C3	C2A6	1.48(4)

Tb1	O3 ⁴	2.338(7)	C3	C2A	1.27(4)
Tb1	O3 ⁵	2.338(7)	C4	C5	1.367(9)
Tb1	O4	2.52(3)	C4	C6	1.487(10)
Tb1	O1A	2.257(12)	C2A	C2A6	0.64(8)
Tb1	O1A1	2.257(12)	C2A	C1A	1.62(7)
Tb1	O4A	2.467(19)	C2A	C1A6	1.76(6)
Tb1	O4A1	2.467(19)	C1A	C1A6	0.76(8)
O1	C1	1.26(3)	C1A	O1A	1.23(4)
O2	C6	1.216(11)	C1A	O1A6	1.47(5)
O3	C6	1.216(10)	O4A	O4A1	1.74(8)
C1	C2	1.41(8)			

¹1+Y,-1+X,3/4-Z; ²1-Y,-X,5/4-Z; ³1-X,-Y,-1/2+Z; ⁴+Y,-X,-1/4+Z; ⁵1-X,-1+Y,1-Z; ⁶1-X,+Y,1-Z

Table S3. Crystal data and structure refinement for TbBTC-b.

Empirical formula	C ₂₇ H ₁₅ O ₂₁ Tb ₃
Formula weight	1152.15
Temperature/K	170.00(10)
Crystal system	tetragonal
Space group	P4 ₃ 22
a/Å	10.2107(2)
b/Å	10.2107(2)
c/Å	43.1372(13)
α/°	90
β/°	90
γ/°	90
Volume/Å ³	4497.4(2)
Z	4
ρ _{calc} /cm ³	1.702
μ/mm ⁻¹	4.732
F(000)	2160.0
Crystal size/mm ³	0.35 × 0.11 × 0.07
Radiation	MoKα (λ = 0.71073)
2θ range for data collection/°	3.776 to 60.71
Index ranges	-13 ≤ h ≤ 13, -10 ≤ k ≤ 13, -60 ≤ l ≤ 53
Reflections collected	29168
Independent reflections	6144 [R _{int} = 0.0585, R _{sigma} = 0.0561]
Data/restraints/parameters	6144/168/234
Goodness-of-fit on F ²	1.130
Final R indexes [I ≥ 2σ (I)]	R1 = 0.0575, wR2 = 0.1272

Final R indexes [all data]	R1 = 0.0619, wR2 = 0.1285
Largest diff. peak/hole / e Å ⁻³	2.43/-2.33
Flack parameter	0.14(4)

Table S4. Bond Lengths for TbBTC-b.

Atom	Atom	Length/Å	Atom	Atom	Length/Å
Tb1	O1	2.303(14)	O6	C7	1.278(15)
Tb1	O4	2.251(12)	O7	C12	1.263(14)
Tb1	O6	2.347(9)	O8	C13	1.222(16)
Tb1	O7	2.301(10)	O9	C13 ²	1.183(18)
Tb1	O8	2.281(10)	C1	C2	1.525(19)
Tb1	O9	2.293(14)	C2	C3	1.386(17)
Tb1	O11	2.427(10)	C2	C4	1.356(18)
Tb2	O2	2.319(10)	C4	C5	1.411(16)
Tb2	O2 ¹	2.319(10)	C5	C12 ³	1.47(3)
Tb2	O3 ¹	2.23(2)	C6	C10 ⁴	1.57(3)
Tb2	O3	2.23(2)	C7	C8	1.485(17)
Tb2	O5	2.383(11)	C8	C9	1.361(19)
Tb2	O5 ¹	2.383(11)	C8	C11	1.368(19)
Tb2	O10	2.35(2)	C9	C10	1.37(2)
O1	C1	1.23(2)	C10	C15 ⁵	1.42(2)
O2	C1	1.222(18)	C11	C14 ⁵	1.374(17)
O3	C6	1.26(3)	C13	C14	1.492(17)
O4	C6	1.22(2)	C14	C15	1.38(2)
O5	C7	1.278(16)			

¹-1+Y,1+X,1/4-Z; ²-X,+Y,-Z; ³+X,1+Y,+Z; ⁴+Y,1+X,1/4-Z; ⁵-1+Y,1-X,1/4+Z

Table S5. Crystal data and structure refinement for TbBTC-c.

Empirical formula	C ₉ H ₅ O ₇ Tb
Formula weight	384.06
Temperature/K	169.97(10)
Crystal system	tetragonal
Space group	P4 ₃ 22
a/Å	10.2191(2)
b/Å	10.2191(2)
c/Å	14.3738(5)
α/°	90

$\beta/^\circ$	90
$\gamma/^\circ$	90
Volume/ \AA^3	1501.06(8)
Z	4
$\rho_{\text{calc}}/\text{cm}^3$	1.699
μ/mm^{-1}	23.354
F(000)	720.0
Crystal size/ mm^3	$0.2 \times 0.05 \times 0.05$
Radiation	CuK α ($\lambda = 1.54184$)
2 θ range for data collection/ $^\circ$	8.652 to 150.33
Index ranges	$-12 \leq h \leq 11, -12 \leq k \leq 12, -16 \leq l \leq 17$
Reflections collected	7117
Independent reflections	1490 [Rint = 0.0611, Rsigma = 0.0280]
Data/restraints/parameters	1490/36/104
Goodness-of-fit on F ²	1.178
Final R indexes [$I \geq 2\sigma(I)$]	R1 = 0.0536, wR2 = 0.1210
Final R indexes [all data]	R1 = 0.0576, wR2 = 0.1272
Largest diff. peak/hole / e \AA^{-3}	1.061/-0.900
Flack parameter	0.11(3)

Table S6. Bond Lengths for TbBTC-c.

Atom	Atom	Length/ \AA	Atom	Atom	Length/ \AA
Tb1	O1 ¹	2.339(13)	O3	C6	1.36(3)
Tb1	O1 ²	2.339(13)	C2	C3	1.41(3)
Tb1	O2 ³	2.35(2)	O4	O4 ³	0.87(5)
Tb1	O2	2.35(2)	C1	C2 ⁴	1.399(16)
Tb1	O3 ³	2.24(2)	C1	C2	1.399(16)
Tb1	O3	2.24(2)	C1	C6 ⁵	1.52(3)
Tb1	O4	2.44(2)	C2	C3	1.377(19)
Tb1	O4 ³	2.44(2)	C3	C4	1.358(18)
Tb1	O2A	2.32(3)	C3	C5	1.51(2)
Tb1	O2A ³	2.32(3)	C4	C5	1.367(9)
Tb1	O3A	2.33(2)	C5	C2A	1.44(4)
Tb1	O3A ³	2.33(2)	C6	C3A	1.23(2)
O1	C5	1.20(2)	C6	C3A ⁶	1.23(2)
O2	C5	1.14(3)			

¹-X,Y,-Z+1; ²-Y+1,X+1,Z-1/4; ³-Y+1,-X+1,-Z+3/4; ⁴X,-Y+2,-Z+3/2; ⁵-X+1,-Y+2,Z+1/2; ⁶X,-Y+2,-Z+1/2; ⁷Y-1,-X+1,Z+1/4; ⁸-X+1,-Y+2,Z-1/2

Table S7. Crystal data and structure refinement for TbBTC-d.

Empirical formula	C ₂₇ H ₁₅ O ₂₁ Tb ₃
Formula weight	1152.15
Temperature/K	170.00(10)
Crystal system	tetragonal
Space group	P4 ₁ 22
a/Å	10.22870(10)
b/Å	10.22870(10)
c/Å	43.1650(6)
α /°	90
β /°	90
γ /°	90
Volume/Å ³	4516.20(11)
Z	4
ρ calc/cm ³	1.695
μ /mm ⁻¹	23.287
F(000)	2160.0
Crystal size/mm ³	0.3 × 0.06 × 0.05
Radiation	CuK α (λ = 1.54184)
2 θ range for data collection/°	8.194 to 150.874
Index ranges	-12 ≤ h ≤ 12, -9 ≤ k ≤ 12, -42 ≤ l ≤ 54
Reflections collected	21640
Independent reflections	4577 [Rint = 0.0420, Rsigma = 0.0280]
Data/restraints/parameters	4577/36/245
Goodness-of-fit on F ²	1.071
Final R indexes [$I \geq 2\sigma(I)$]	R1 = 0.0636, wR2 = 0.1629
Final R indexes [all data]	R1 = 0.0655, wR2 = 0.1645
Largest diff. peak/hole / e Å ⁻³	1.98/-1.73
Flack parameter	0.12(2)

Table S8. Bond Lengths for TbBTC-d.

Atom Atom	Length/Å	Atom Atom	Length/Å
Tb1 O1	2.22(2)	O5 C15	1.20(2)
Tb1 O1 ¹	2.22(2)	O6 C15	1.30(2)
Tb1 O5 ²	2.393(12)	O7 C25	1.273(15)
Tb1 O5 ³	2.393(12)	O8 C20	1.24(2)
Tb1 O8 ⁴	2.303(12)	O9 C20	1.20(2)
Tb1 O8 ⁵	2.303(12)	C3 C4	1.40(2)
Tb1 O11	2.41(3)	C3 C8	1.39(2)

Tb1	O1A1	2.33(3)	C3	C9	1.54(3)
Tb1	O1A	2.33(3)	C4	C5	1.36(2)
Tb2	O2	2.246(13)	C5	C6	1.37(2)
Tb2	O3 ⁶	2.276(12)	C5	C15	1.50(2)
Tb2	O4 ²	2.315(14)	C6	C7	1.38(2)
Tb2	O6 ³	2.332(14)	C7	C8	1.40(2)
Tb2	O7	2.276(12)	C7	C12	1.50(2)
Tb2	O9 ⁵	2.318(14)	C9	O1A	1.30(3)
Tb2	O10	2.405(14)	C20	C22	1.52(2)
O1	C9	1.32(3)	C22	C23	1.34(2)
O2	C9	1.23(2)	C22	C27	1.419(19)
O3	C12	1.21(2)	C23	C24	1.414(18)
O4	C12	1.17(2)	C24	C25	1.46(3)

¹-Y,-X,5/4-Z; ²+X,-1+Y,+Z; ³1-Y,-X,5/4-Z; ⁴+Y,1-X,-1/4+Z; ⁵-1+X,-Y,3/2-Z; ⁶+X,1-Y,3/2-Z

Table S9. Crystal data and structure refinement for DSM@P-(+)-TbBTC after removing the DSM molecule.

Empirical formula	C ₉ H ₅ O ₇ Tb
Formula weight	384.05
Temperature/K	272.98(13)
Crystal system	tetragonal
Space group	P4 ₁ 22
a/Å	10.3134(3)
b/Å	10.3134(3)
c/Å	14.4191(6)
α/°	90
β/°	90
γ/°	90
Volume/Å ³	1533.71(11)
Z	4
ρ _{calc} /cm ³	1.663
μ/mm ⁻¹	22.857
F(000)	720.0
Crystal size/mm ³	0.25 × 0.24 × 0.14
Radiation	CuKα (λ = 1.54184)
2θ range for data collection/°	10.546 to 149.31
Index ranges	-12 ≤ h ≤ 12, -8 ≤ k ≤ 12, -17 ≤ l ≤ 17
Reflections collected	9452

Independent reflections	1557 [Rint = 0.0429, Rsigma = 0.0212]
Data/restraints/parameters	1557/12/80
Goodness-of-fit on F ²	1.094
Final R indexes [I>=2σ (I)]	R1 = 0.0289, wR2 = 0.0753
Final R indexes [all data]	R1 = 0.0290, wR2 = 0.0753
Largest diff. peak/hole / e Å ⁻³	0.56/-0.97
Flack parameter	-0.031(9)

Table S10. Bond Lengths for DSM@P-(+)-TbBTC after removing the DSM molecule.

Atom	Atom	Length/Å	Atom	Atom	Length/Å
Tb1	O1 ¹	2.304(5)	O2	C5	1.261(9)
Tb1	O1	2.304(5)	O3	C5	1.228(9)
Tb1	O2 ²	2.320(5)	C1	C2	1.495(12)
Tb1	O2 ³	2.320(5)	C2	C3 ⁶	1.402(8)
Tb1	O3 ⁴	2.306(5)	C2	C3	1.403(8)
Tb1	O3 ⁵	2.306(5)	C3	C4	1.386(10)
Tb1	O4	2.461(9)	C4	C5	1.493(9)
O1	C1	1.250(7)	C4	C6	1.390(8)

¹+Y,+X,3/4-Z; ²-X,1-Y,-1/2+Z; ³1-Y,-X,5/4-Z; ⁴-X,-1+Y,1-Z; ⁵-1+Y,-X,-1/4+Z; ⁶-X,+Y,1-Z

Table S11. Crystal data and structure refinement for DSM.

Empirical formula	C ₁₆ H ₁₉ IN ₂
Formula weight	366.23
Temperature/K	170.00(10)
Crystal system	monoclinic
Space group	P2 ₁ /c
a/Å	6.28820(10)
b/Å	7.61980(10)
c/Å	32.0146(4)
α/°	90
β/°	90.1460(10)
γ/°	90
Volume/Å ³	1533.97(4)
Z	4
ρ _{calc} /cm ³	1.586
μ/mm ⁻¹	16.297

F(000)	728.0
Crystal size/mm ³	0.3 × 0.3 × 0.05
Radiation	CuK α (λ = 1.54184)
2 θ range for data collection/°	5.52 to 150.816
Index ranges	-6 ≤ h ≤ 7, -9 ≤ k ≤ 9, -36 ≤ l ≤ 40
Reflections collected	9183
Independent reflections	3045 [Rint = 0.0449, Rsigma = 0.0317]
Data/restraints/parameters	3045/0/175
Goodness-of-fit on F2	1.091
Final R indexes [$I \geq 2\sigma(I)$]	R1 = 0.0440, wR2 = 0.1144
Final R indexes [all data]	R1 = 0.0445, wR2 = 0.1152
Largest diff. peak/hole / e Å ⁻³	0.82/-1.92

Table S12. Bond Lengths for DSM.

Atom	Atom	Length/Å	Atom	Atom	Length/Å
N1	C1	1.370(4)	C4	C5	1.408(4)
N1	C1	1.449(4)	C4	C9	1.451(4)
N1	C8	1.454(4)	C5	C6	1.380(4)
N2	C13	1.335(5)	C9	C10	1.351(5)
N2	C14	1.353(4)	C10	C11	1.439(5)
N2	C16	1.476(4)	C11	C12	1.415(4)
C1	C2	1.419(4)	C11	C15	1.404(5)
C1	C6	1.414(4)	C12	C13	1.372(5)
C2	C3	1.368(5)	C14	C15	1.368(5)
C3	C4	1.414(4)			

Table. S13 The C and N contents in DSM@TbBTC-X determined by Element Analysis.

Sample	N (y ₁ , wt%)	C (x ₁ , wt%)	N(y, mol)	C(x, mol)
S-1	0.006	25.895	4.29E-04m	2.158m
S-2	0.012	26.474	8.57E-04m	2.206m
S-3	0.014	25.358	1.00 E-03m	2.113m
S-4	0.040	24.596	2.86E-03m	2.050m
S-5	0.065	24.113	4.64 E-03m	2.009m
DSM@TbBTC	0.366	24.790	2.61 E-02m	2.066m

Note: m represents the mass of DSM@TbBTC-X.

Table. S14 Fluorescent lifetimes, energy transfer efficiency, quantum yield and CIE coordinates of TbBTC and DSM@TbBTC-X

Sample	τ_1 (s)	τ_2 (s)	Average Life Time(s)	Energy transfer	Quantum Yield	CIE coordinates
TbBTC			1.37E-03		41.38	(0.27, 0.56)
X= 1	2.45E-05	2.09E-06	1.15E-03	16.1%	23.84	(0.37, 0.51)
X= 2	1.30E-05	1.96E-06	9.90E-04	27.7%	16.91	(0.45, 0.45)
X= 3	9.49E-06	1.98E-06	9.2E-04	32.8%	17.58	(0.51, 0.42)
X= 4	7.12E-06	2.58E-06	7.12E-04	48.2%	17.04	(0.59, 0.37)
X= 5	6.31E-06	2.88E-06	6.07E-04	55.7%	14.75	(0.61, 0.37)